

# Microscale frictional response of bovine articular cartilage from atomic force microscopy

Seonghun Park, Kevin D. Costa, Gerard A. Ateshian\*

Departments of Mechanical Engineering and Biomedical Engineering, Columbia University, 500 West 120th St, MC4703, 220 S.W. Mudd, New York, NY 10027, USA

Accepted 11 February 2004

## Abstract

The objective of this study was to compare micro- and macroscale friction coefficients of bovine articular cartilage. Microscale measurements were performed using standard atomic force microscopy (AFM) techniques, using a 5  $\mu\text{m}$  spherical probe tip. Twenty-four cylindrical osteochondral plugs were harvested in pairs from adjacent positions in six fresh bovine humeral heads (4–6 months old), and divided into two groups for AFM and macroscopic friction measurements. AFM measurements of friction were observed to be time-independent, whereas macroscale measurements demonstrated the well-documented time-dependent increase from a minimum to an equilibrium value. The microscale AFM friction coefficient ( $\mu_{\text{AFM}}$ ,  $0.152 \pm 0.079$ ) and macroscale equilibrium friction coefficient ( $\mu_{\text{eq}}$ ,  $0.138 \pm 0.036$ ) exhibited no statistical differences ( $p = 0.50$ ), while the macroscale minimum friction coefficient ( $\mu_{\text{min}}$ ,  $0.004 \pm 0.001$ ) was significantly smaller than  $\mu_{\text{eq}}$  and  $\mu_{\text{AFM}}$  ( $p < 0.0001$ ). Variations in articular surface roughness ( $R_q = 462 \pm 216$  nm) did not correlate significantly with  $\mu_{\text{AFM}}$ ,  $\mu_{\text{eq}}$  or  $\mu_{\text{min}}$ . The effective compressive modulus determined from AFM indentation tests using a Hertz contact analysis was  $E^* = 45.8 \pm 18.8$  kPa. The main finding of this study is that  $\mu_{\text{AFM}}$  is more representative of the macroscale equilibrium friction coefficient, which represents the frictional response in the absence of cartilage interstitial fluid pressurization. These results suggest that AFM measurements may be highly suited for exploring the role of boundary lubricants in diarthrodial joint lubrication independently of the confounding effect of fluid pressurization to provide greater insight into articular cartilage lubrication.

© 2004 Elsevier Ltd. All rights reserved.

**Keywords:** Atomic force microscopy (AFM); Cartilage mechanics; Friction coefficient; AFM indentation

## 1. Introduction

Atomic force microscopy (AFM) techniques are increasingly used for tribological studies of engineering and biological surfaces at nanoscale and microscale levels (Bhushan, 1995b; Kumar et al., 2001). Microscale tribological and mechanical material properties such as surface roughness, wear, friction, elastic modulus, and boundary lubrication have been studied on engineering and biological surfaces by AFM (Bhushan and Koinkar, 1996; Du et al., 2001). However, the tribological and mechanical material properties of articular cartilage have not yet been well characterized at microscale levels, neither have the relationships

between microscale properties or between micro- and macroscale properties. In this study we report surface roughness ( $R_q$ ), effective modulus ( $E^*$ ), micro- and macroscale frictional coefficients, and their relationships, in bovine humeral head articular cartilage using AFM techniques.

According to previous AFM studies of microscale structure, the surface of articular cartilage exhibits a fibrillar structure, an amorphous structure, and a mix of these two structures (Jurvelin et al., 1996; Kumar et al., 2001; Moa-Anderson et al., 2003). In addition, the surface roughness ( $R_a$ ) of immature bovine humeral head articular cartilage, scanned over a  $100 \times 100 \mu\text{m}$  area, has been determined from AFM to be  $\sim 0.5 \mu\text{m}$  (Moa-Anderson et al., 2003). With regard to microscale mechanical properties of soft materials, AFM indentation testing has been widely used to calculate Young's modulus ( $E_Y$ ) from Hertz contact models (A-Hassan

\*Corresponding author. Tel.: +1-212-854-8602; fax: +1-212-854-3304.

E-mail address: ateshian@columbia.edu (G.A. Ateshian).

et al., 1998; Costa and Yin, 1999; Heinz and Hoh, 1999; Mathur et al., 2000, 2001). However there is limited AFM data for articular cartilage; Young's modulus ( $E_Y$ ) of rabbit jaw condylar articular cartilage has been compared between neonatal ( $\sim 0.9$ – $1$  MPa) and adult tissue ( $\sim 1$ – $2$  MPa) (Hu et al., 2001; Patel and Mao, 2003). Many AFM studies have used a small and sharp AFM probe for indentation testing. Dimitriadis and co-workers have shown that spherical AFM cantilever probes can reduce the nonlinearity of soft materials compared to sharp cantilever probes (Tymiak et al., 2001; Dimitriadis et al., 2002).

At microscale levels, AFM friction studies have been reported on many biological surfaces such as hydrogels, phospholipid co-adsorbed layers onto hydrophobic and hydrophilic solid supports, dentin, enamel, dentino-enamel junction, and human hair with various surface modifications (Gong et al., 1999; Habelitz et al., 2001; Kim et al., 2001; McMullen and Kelty, 2001; Grant and Tiberg, 2002; Kim et al., 2002). Frictional forces consist mainly of adhesion forces, elastic forces from elastic deformation, and plowing forces from inelastic deformation. Plowing forces should be reduced in order to obtain a constant frictional coefficient without being influenced by the amount of applied normal loads (Suh and Sin, 1981). Habelitz et al., have used a relatively large spherical cantilever probe ( $10\ \mu\text{m}$  radius) with the amount of applied normal loads in the range of  $\sim 50$ – $600\ \mu\text{N}$  to minimize plowing forces from plastic deformation, and found that frictional coefficients of intertubular dentin and enamel were  $\sim 0.31$  and  $\sim 0.14$ , respectively (Habelitz et al., 2001). Many studies of the frictional coefficient of articular cartilage have been reported at the macroscale level (Mow and Ateshian, 1997), but to the best of our knowledge, the frictional coefficient of articular cartilage has not been reported at the microscale. Some investigators have proposed that articular cartilage can achieve very low frictional coefficients at macroscale levels because its interstitial water can support most of the applied load upon initial load application; however, under a constant applied load, the interstitial fluid pressure will slowly subside, resulting in a concomitant time-dependent increase in the friction coefficient, eventually reaching an equilibrium value (McCutchen, 1962; Forster and Fisher, 1996; Ateshian, 1997; Ateshian et al., 1998; Krishnan et al., 2003). Measurements of the frictional response of articular cartilage at the microscale may yield valuable insight into the frictional response of the tissue and the mechanisms responsible for its remarkable tribological properties. The objective of the present study was to compare micro- and macroscale frictional coefficients of bovine articular cartilage by using a relatively large AFM spherical probe tip and applying previously reported methodologies (Ruan and Bhushan, 1994; Bhushan, 1995a).

## 2. Materials and methods

### 2.1. Sample preparation

Twenty-four cylindrical osteochondral plugs were harvested in pairs from adjacent locations in six fresh bovine humeral heads (4–6 months old), and divided into two groups for AFM ( $\varnothing 8\ \text{mm}$ ,  $h = 1.58 \pm 0.17\ \text{mm}$ ) and macroscopic ( $\varnothing 4.78\ \text{mm}$ ,  $h = 1.66 \pm 0.24\ \text{mm}$ ) measurements. Using a sledge microtome (Model 1400; Leiz, Rockleigh, NJ), approximately 1 mm of the tissue for AFM and 0.5 mm of the tissue for macroscale friction measurements were removed from the deep zone to remove remnants of subchondral bone and vascularized tissue and produce a surface parallel to the articular side, leaving the articular surface intact. All samples were refrigerated at  $4^\circ\text{C}$  and tested within 3 days, but never frozen.

### 2.2. AFM measurements

Samples in the AFM group were glued on the bony side to 35 mm polystyrene petri dishes using a small amount of cyanoacrylate glue. Frictional signal (trace and retrace) imaging and height imaging were conducted with samples entirely submerged in physiological-buffered saline (PBS) on a Bioscope AFM (Digital Instruments, Santa Barbara, CA) with an extended Z-range of  $12\ \mu\text{m}$ . Custom silicon-nitride AFM probes with polystyrene  $\varnothing 5\ \mu\text{m}$  spherical tips (Novascan Technologies, Ames, IA) having a nominal spring constants of  $k = 0.32\ \text{N/m}$  were used. The mounted probe was submerged in PBS for at least 20 min prior to imaging to allow for thermal equilibration at room temperature.

Friction was measured under a constant load using a  $90^\circ$  scan angle (Meyer and Amer, 1990); the sample was moved in the direction perpendicular to the cantilever long axis, at a velocity of  $200\ \mu\text{m/s}$  in a raster scan mode to cover a  $100 \times 100\ \mu\text{m}$  area ( $128 \times 128$  pixels) over 128 s. The friction voltage signal was averaged over the scanned area for both trace and retrace scans, using the Nanoscope III software shipped with the microscope (Digital Instruments, Santa Barbara, CA) (Fig. 1). Half of the difference between tracing and retracing voltage signals was calculated, which represents a measure of the pure friction signal; this voltage was converted to units of force using a conversion factor based on a calibration test performed on platinum, following published methods (Ruan and Bhushan, 1994; Bhushan, 1995a). Friction measurements were repeated for five incremental values of normal force in the range of 25–100 nN, obtained by altering the set-point voltage in five consecutive scans. Ascending or descending force increments were randomly selected for each test location.

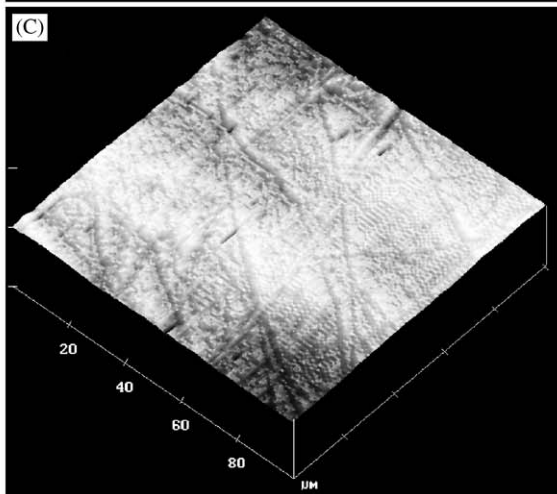
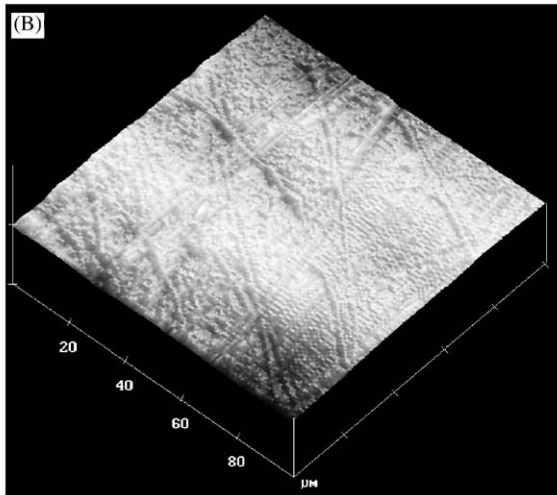
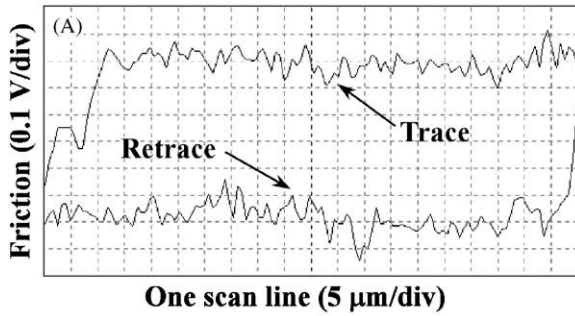


Fig. 1. (A) Typical profile of the frictional voltage signal, as a sample is scanned back and forth in the direction perpendicular to the cantilever beam. Trace (B) and retrace (C) frictional voltage signal over the  $100 \times 100 \mu\text{m}$  test area (vertical range = 10 V) showing the fibrillar structure of articular cartilage.

The normal force was determined from the net normal deflection voltage of the cantilever probe, which was converted to units of force using the AFM deflection sensitivity determined in PBS on glass and  $k$  of the cantilever beam.

Measurement of the frictional force was repeated for the five step increments of normal load at a given

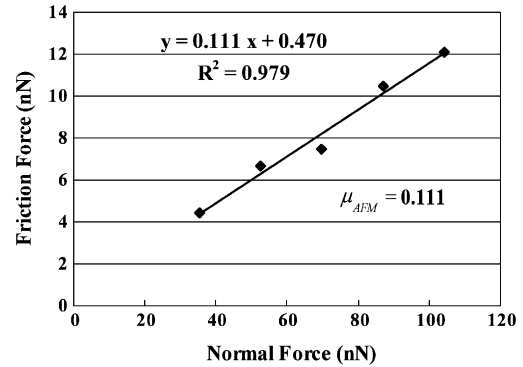


Fig. 2. Typical plot of AFM frictional force versus normal load over five load increments, with the slope yielding  $\mu_{AFM}$ .

location. The friction versus normal force response was fitted with a straight line whose slope is the frictional coefficient ( $\mu_{AFM}$ , Fig. 2). The surface roughness ( $R_q$ ) was measured over the same  $100 \times 100 \mu\text{m}$  test area from the height image obtained simultaneously. The applied stress and effective modulus were also estimated, from an additional indentation test at the same location, using a Hertz contact model. Each series of friction and indentation measurements was repeated at three different surface locations on each cartilage sample ( $n = 3 \times 12 = 36$ ).

### 2.3. Macroscopic measurements

Macroscopic frictional measurements were performed on the paired cartilage samples using a custom friction device (Krishnan et al., 2003). Sliding motion ( $200 \mu\text{m/s}$ ) was provided by a computer-controlled translation stage (Model PM500-1L, Newport Corporation, Irvine, CA). Normal loads (3.6 N, 200 kPa) were prescribed via a voice-coil force actuator (Model LA17-28-000A; BEI Kimco Magnetics Division, San Marcos, CA) connected in series with an LVDT for displacement measurements (Model PR812-200, Schaeviz Sensors, Hamptons, VA). The voice-coil force actuator, connected to a power supply (Model PST-040-13-DP, Copley Controls Corp., Canton, MA) and controller box (Model TA115, Trust Automation INC., San Luis Obispo, CA) was controlled via a force feedback loop using a desktop computer, via LabView software (National Instruments, Austin, TX). All loads were measured with a multiaxial load cell mounted on the translation stage (Model 20E12A-M25B, JR3 Inc., Woodland, CA). Specimens were loaded using a polystyrene platen (same material as the AFM probe tip). From the measured time-dependent normal and frictional force, the minimum ( $\mu_{\min}$ ) and equilibrium ( $\mu_{\text{eq}}$ ) frictional coefficient were calculated (Fig. 3).

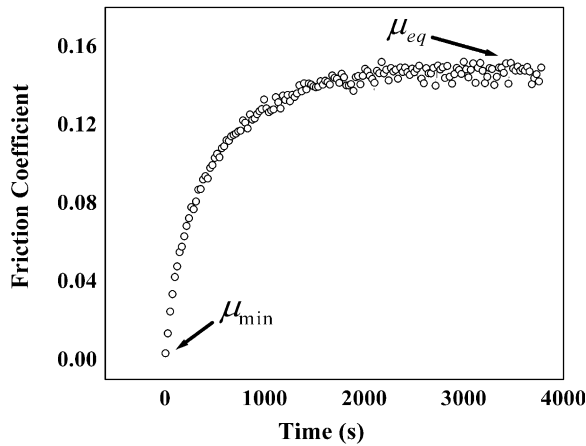


Fig. 3. Typical time-dependent response of the macroscopic friction coefficient, showing  $\mu_{\min}$  and  $\mu_{\text{eq}}$ .

#### 2.4. Analysis of surface roughness measurement and indentation test

Surface topography measurements were acquired with the same AFM probe (Fig. 4). Surface roughness ( $R_q$ ) was calculated from the topography, using Nanoscope III software, by root mean square averaging of height deviations over the  $100 \times 100 \mu\text{m}$  scan area ( $128 \times 128$  pixels) at each location, with  $R_q = \sqrt{\sum_{i=1}^N Z_i^2 / N}$ , where  $Z_i$  is the height deviation from the mean plane and  $N$  is the number of pixels over the scanned area. In order to estimate the mean applied stress ( $p_m$ ) and effective modulus ( $E^*$ ) using Hertz contact analysis, the approach signals from indentation tests were converted to indentation depth ( $D=Z-h$ ) versus indentation load curves, where  $Z$  is the sample position height, and  $h$  is the cantilever deflection (Fig. 5).

The applied normal load ( $F$ ) of AFM friction measurements ranged from  $29.5 \pm 3.1$  to  $98.4 \pm 3.1$  nN. For the measurement of the elastic modulus using a Hertz contact analysis, indentation loads were applied up to 41.6 nN ( $= 13 \text{ nm/div} \times 10 \text{ div} \times 0.32 \text{ nN/nm}$ ) (Fig. 5A). The indentation depth versus normal load data were fitted to the Hertz contact formula  $F = (4/3)E^*R^{1/2}D^{3/2}$ , with  $R = 2.5 \mu\text{m}$  (Fig. 5B) (Johnson, 1985; Radmacher, 2002). The effective modulus ( $E^*$ ), which relates to Young's modulus ( $E_Y$ ) and Poisson's ratio ( $\nu$ ) through  $E^* = E_Y / (1 - \nu^2)$ , was then evaluated from this relation and the applied mean stress ( $p_m$ ) obtained from  $p_m = (2/3)(6FE^*2/\pi^3R^2)^{1/3}$ .

These normal force measurements were also used to estimate adhesion forces between the AFM probe's polystyrene spherical tip and the cartilage surface. Adhesion forces were more evident during probe retraction (Fig. 5A), where they can be identified as the dip below the baseline deflection in the non-contact regime. Using linear regression on the baseline signal to

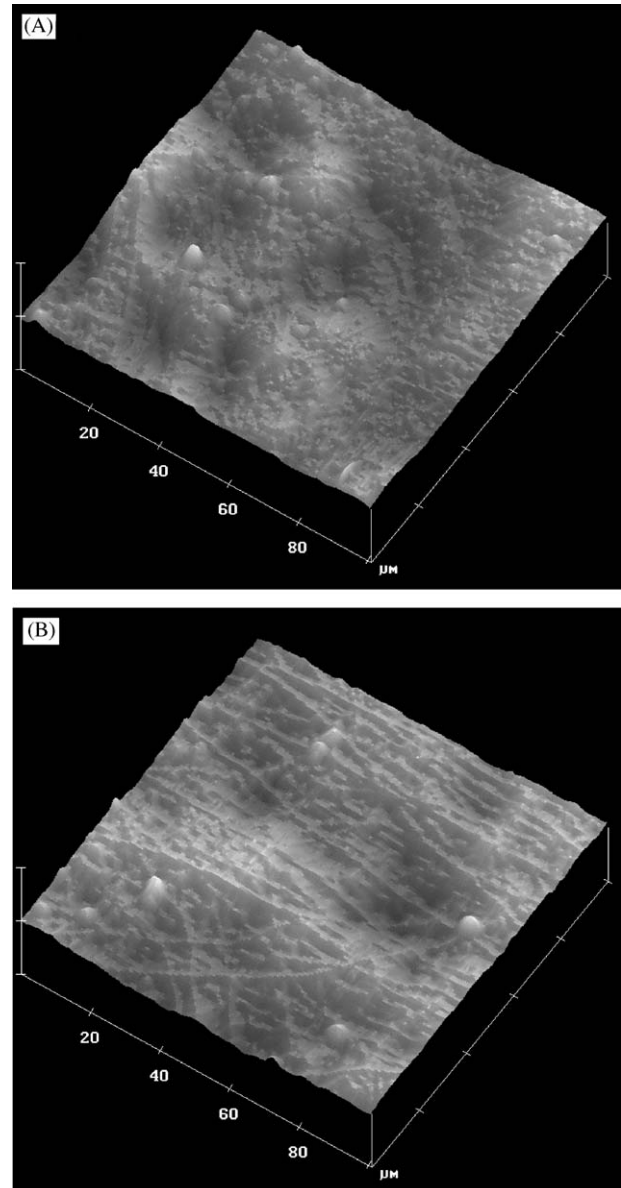


Fig. 4. AFM height images, acquired with spherical  $\varnothing 5 \mu\text{m}$  probe, indicates that the fine surface structure of the bovine articular surface may exhibit either amorphous (A) or fibrillar (B) structures, depending on location. ( $Z$  scale =  $10 \mu\text{m}$ . A:  $R_q = 262 \text{ nm}$  and  $\mu_{\text{AFM}} = 0.280$ ; B:  $R_q = 292 \text{ nm}$  and  $\mu_{\text{AFM}} = 0.119$ )

identify a suitable reference for zero contact force, the maximum adhesion force was estimated from the lowest “dipping” point below the baseline. This force was measured at  $4.29 \pm 2.19$  nN for the retracting trace and  $0.14 \pm 0.07$  nN for the approaching trace. In comparison, the periodic fluctuation in the non-contact regime (most likely due to laser interference) produced a noise signal equivalent to  $\sim 0.19$  nN. This result confirms that there was negligible adhesion during approach, which facilitates the interpretation of frictional measurements and permits the use of a Hertz contact analysis.

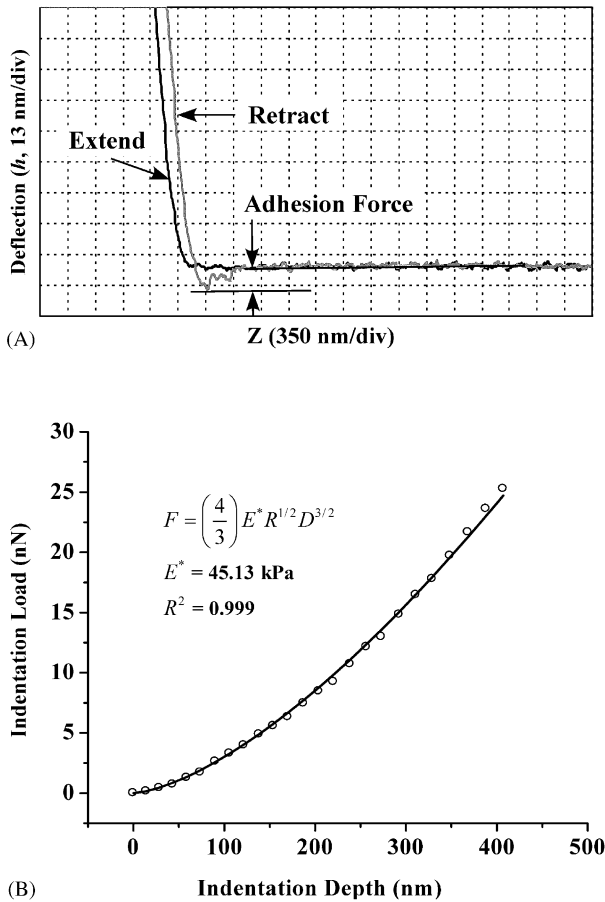


Fig. 5. Typical profile of approaching and retracting signals from indentation tests (A) with corresponding conversion to indentation depth ( $D=Z-h$ ) versus indentation load (B). The periodic force component in the non-contact regime in (A) is likely due to laser interference.

2.5. Statistical analyses

One-way ANOVA with repeated measures was performed to investigate statistical differences between  $\mu_{min}$ ,  $\mu_{eq}$ , and  $\mu_{AFM}$  (SAS Institute Inc., Cary, NC) with an  $\alpha=0.05$ . Post-hoc testing of means was performed using Bonferroni adjustments.

2.6. Effect of scan area and sliding speed

Measurements were performed on an additional set of three cartilage specimens to explore the influence of scan area and sliding speed on the measurement of  $\mu_{AFM}$ . In the first series of tests, the friction coefficient was obtained for scan areas of  $100 \times 100$ ,  $50 \times 50$ , and  $25 \times 25 \mu\text{m}$  at a constant sliding speed of  $200 \mu\text{m/s}$  at nine locations on the cartilage samples. In the second series of tests,  $\mu_{AFM}$  was measured at sliding speeds of 100, 200, and  $800 \mu\text{m/s}$  over a  $100 \times 100 \mu\text{m}$  scan area, at nine locations on the same samples. One-way ANOVA was used in each series of tests to analyze statistical differences.

3. Results

The frictional response at the microscale was found to remain nearly constant during the entire 128 s scan, as shown in a representative plot of the friction force averaged over each of the 128 consecutive scan lines (Fig. 6). Average  $\pm$  standard deviation values of the microscale AFM frictional coefficient calculated from the linear fit of friction versus normal force was  $\mu_{AFM} = 0.152 \pm 0.079$  with  $R^2 = 0.957 \pm 0.024$  ( $n = 3 \times 12 = 36$ , Fig. 7). In contrast, the frictional response at the macroscale was time-dependent, increasing from a minimum value of  $\mu_{min} = 0.004 \pm 0.001$  to an equilibrium value of  $\mu_{eq} = 0.138 \pm 0.036$  ( $n = 12$ , Fig. 7), over a duration of  $3433 \pm 615 \text{ s}$  (Fig. 3).  $\mu_{AFM}$  and  $\mu_{eq}$  exhibited no statistical differences ( $p = 0.50$ ), however  $\mu_{min}$  was significantly smaller than  $\mu_{eq}$  ( $p < 0.0001$ ) and  $\mu_{AFM}$  ( $p < 0.0001$ ).

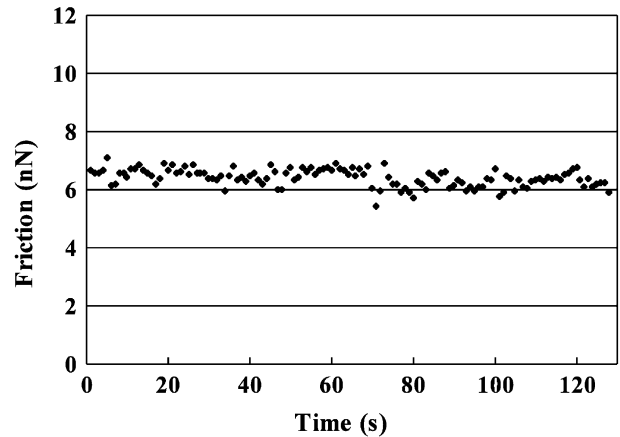


Fig. 6. Typical variation in the frictional force  $F$  measured from AFM over 128 consecutive raster scans covering a  $128 \times 128$  pixel ( $100 \times 100 \mu\text{m}$ ) region. Each data point represents the average friction force over the scan and rescan of a 128 pixel ( $100 \mu\text{m}$ ) line.

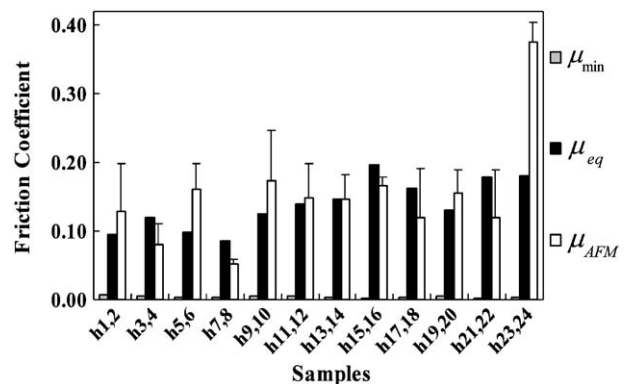


Fig. 7. Friction coefficients from microscale AFM ( $\mu_{AFM}$ ) and macroscale experiments ( $\mu_{min}$  and  $\mu_{eq}$ ), for each specimen pair. AFM results are presented as mean  $\pm$  standard deviation of measurements performed at three locations on each sample.

The surface roughness ( $R_q$ ) was  $462 \pm 216$  nm ( $n = 3 \times 12 = 36$ ) over the same  $100 \times 100 \mu\text{m}$  region where  $\mu_{\text{AFM}}$  was measured. There was no significant correlation between  $R_q$  and  $\mu_{\text{min}}$ ,  $\mu_{\text{eq}}$ , or  $\mu_{\text{AFM}}$  ( $R^2 = 0.03$ , 0.00, and 0.11, respectively).

The effective modulus determined by the Hertz contact model (Fig. 5B) was  $E^* = 45.8 \pm 18.8$  kPa ( $F$  versus  $D$ ,  $R^2 = 0.998 \pm 0.001$ ,  $n = 3 \times 3 \times 12 = 108$ ). From the measured properties, the applied mean contact stress during the AFM friction tests ( $p_m$ ,  $n = 3 \times 3 \times 12 = 108$ ) was estimated to range from  $8.0 \pm 2.1$  to  $12.1 \pm 3.2$  kPa across the five increments of applied normal loads.

From measurements on a smaller set of three cartilage specimens, no statistical difference was found in  $\mu_{\text{AFM}}$  between the  $100 \times 100 \mu\text{m}$  ( $0.165 \pm 0.025$ ) and  $50 \times 50 \mu\text{m}$  ( $0.147 \pm 0.023$ ) scan areas; however  $\mu_{\text{AFM}}$  was significantly smaller ( $p < 0.001$ ) when measured over the  $25 \times 25 \mu\text{m}$  scan area ( $0.105 \pm 0.025$ ).  $\mu_{\text{AFM}}$  was insensitive to changes in sliding speed ( $0.162 \pm 0.032$  at  $100 \mu\text{m/s}$ ,  $0.165 \pm 0.025$  at  $200 \mu\text{m/s}$  and  $0.169 \pm 0.024$  at  $800 \mu\text{m/s}$ ).

The friction force measured in AFM tests was in the range of 3–20 nN. To estimate whether hydrodynamic drag on the spherical probe tip had an influence on these measurements, we can use Stokes' solution for laminar flow around a sphere, since the Reynolds number is very small,  $Re = \rho VD/\eta \approx 10^{-3} \ll 1$  ( $\rho = 1000 \text{ kg/m}^3$ ,  $V = 200 \mu\text{m/s}$ ,  $D = 5 \mu\text{m}$ ,  $\eta = 10^{-3} \text{ Pa}\cdot\text{s}$ ). The resulting hydrodynamic drag force,  $F = 6\pi\eta(D/2)V \approx 0.009 \text{ nN}$ , is found to be negligible.

#### 4. Discussion

The objective of this study was to compare micro- and macroscale frictional coefficients of bovine articular cartilage. Standard AFM techniques for measuring friction and effective modulus at the microscale were found to be successful with articular cartilage (Figs. 1 and 2). The primary finding is that, unlike the macroscale response, the microscale frictional coefficient remains essentially constant over time and that  $\mu_{\text{AFM}}$  is statistically comparable to  $\mu_{\text{eq}}$ . This result suggests that the microscale AFM friction coefficient is a measure of the macroscale equilibrium friction coefficient and not the minimum friction coefficient. This conclusion is reached while recognizing that different stress levels were applied at the microscale ( $\sim 8$ – $12$  kPa) and macroscale (200 kPa) levels.

At the macroscale, the time-dependent frictional response is regulated by the pressurization of the interstitial fluid of cartilage, as hypothesized by several investigators (McCutchen, 1962; Malcom, 1976; Forster and Fisher, 1996; Ateshian, 1997; Ateshian et al., 1998) and confirmed experimentally in our recent studies

(Krishnan et al., 2003). Under a step applied load, the interstitial fluid pressure initially supports the great majority of the load at the contact interface (approaching 100%) (Ateshian et al., 1994; Ateshian and Wang, 1995; Soltz and Ateshian, 1998, 2000a; Park et al., 2003), considerably reducing the component of the contact stress supported by the solid collagen–proteoglycan matrix of cartilage. Consequently, the frictional force produced at the solid-to-solid contact interface is initially very small. With increasing time however, the interstitial fluid flows away from the contact region while the pressure correspondingly subsides at a rate determined primarily by the characteristic size of the contact area, as well as the modulus and permeability of the tissue (Ateshian et al., 1994; Kelkar and Ateshian, 1999). With decreasing interstitial fluid load support, the component of the contact stress supported by the solid matrix increases, with a concomitant increase in the frictional force and friction coefficient, as observed in the representative result of Fig. 3. When the fluid pressure has reduced to zero, all of the contact stress is supported by the solid matrix and the friction coefficient reaches an equilibrium value.

From theoretical analyses based on the biphasic theory for cartilage (Mow et al., 1980), the characteristic time constant for the time-dependent decrease in interstitial fluid load support is proportional to  $a^2/H_A k$ , where  $a$  is the characteristic size (e.g., radius) of the contact area,  $H_A$  is the aggregate modulus of the solid matrix (in tension), and  $k$  is its hydraulic permeability (Armstrong et al., 1984; Ateshian et al., 1994; Kelkar and Ateshian, 1999). Using representative values of the material properties of immature bovine cartilage from our recent study (Soltz and Ateshian, 2000b),  $H_A = 13 \text{ MPa}$  and  $k = 0.6 \times 10^{-15} \text{ m}^4/\text{N}\cdot\text{s}$ , with  $a = 2.39 \text{ mm}$  (the radius of tissue samples in macroscale friction experiments) yields a time constant of 730 s, consistent with the time-dependent response of the macroscopic friction coefficient in Fig. 3. At the microscale however,  $a$  is on the order of  $1 \mu\text{m}$  so that the time constant is on the order of 0.1 ms. Consequently, because of the very small size of the AFM indenter tip, interstitial fluid pressurization will subside very rapidly in AFM friction measurements. In light of this explanation, it is not surprising to find that  $\mu_{\text{AFM}}$  is more representative of  $\mu_{\text{eq}}$  than  $\mu_{\text{min}}$ .

Under physiological loading conditions it is not expected that the friction coefficient will achieve its equilibrium value because joint loading is typically intermittent and the contact region in articular joints is much greater than in the test samples used in this study. (For example, a contact area of  $4 \text{ cm}^2$  in the patellofemoral joint corresponds to  $a \sim 11 \text{ mm}$  and a time constant of  $\sim 4.5 \text{ h}$ , whereas purely static loading conditions rarely exceed a few minutes in vivo.) Consequently,  $\mu_{\text{min}}$  is a more functional measure of the frictional response of articular cartilage.

Nevertheless, knowledge of  $\mu_{\text{eq}}$  (and hence  $\mu_{\text{AFM}}$ ) can be valuable because it represents the intrinsic frictional coefficient of the solid matrix in the absence of interstitial fluid pressurization. If certain components of synovial fluid or articular cartilage, such as lubricin, superficial zone protein, phospholipids, hyaluronan, etc., are effective boundary lubricants (Swann et al., 1985; Flannery et al., 1999; Schumacher et al., 1999; Hills, 2000; Jay et al., 2001), it would be reasonable to expect that they would help reduce the value of  $\mu_{\text{eq}}$ . These findings suggest that AFM measurements of the friction coefficient of articular cartilage may be ideal for identifying the effectiveness of putative boundary lubricants without the confounding effect of interstitial fluid pressurization on the frictional response. Such measurements may be achieved for example by coating the AFM probe and/or cartilage surface with various boundary lubricants to assess their effectiveness. The ability to separately assess the contribution of interstitial fluid pressurization and boundary lubricants in the frictional response of articular cartilage would be valuable, both from a basic science and from a clinical perspective. For example, we currently believe that interstitial fluid pressurization plays a much more significant role in reducing friction at the surface of contacting articular layers. Thus clinical treatment modalities would need to focus on strategies that either prevent or minimize loss of interstitial fluid pressurization during normal physiological loading conditions in cartilage. Alternatively, cartilage tissue engineering may restore the integrity of the articular layers to promote greater interstitial fluid pressurization. Conversely, if boundary lubricants are found to be most effective, then treatment modalities can focus on delivering such lubricants onto the articular surfaces.

In addition to these findings, the surface roughness measured in this study,  $R_q \sim 460$  nm, was essentially the same as reported in our recent study of the surface morphology of immature bovine articular cartilage by AFM (Moa-Anderson et al., 2003) and comparable to measurements with other methods (Forster and Fisher, 1999). No significant relationship between surface roughness ( $R_q$ ) and the micro- or macroscale friction coefficients ( $\mu_{\text{AFM}}$ ,  $\mu_{\text{min}}$ , or  $\mu_{\text{eq}}$ ) was observed, consistent with studies in other materials (Bhushan, 1995a; Poon and Bhushan, 1995). The fine surface structure of the bovine articular cartilage presented in Fig. 4 was observed to be either amorphous or fibrillar, also consistent with previous findings performed at a higher scanning resolution (Jurvelin et al., 1996; Kumar et al., 2001; Moa-Anderson et al., 2003).

The effective compressive modulus of the topmost superficial zone of immature bovine articular cartilage was estimated from the AFM measurements of this study at  $E^* \sim 46$  kPa. While this may seem at first to be a relatively small value when compared to the average

equilibrium compressive modulus of bovine cartilage, it is in fact in good agreement with measurements of the inhomogeneous depth-dependent equilibrium modulus by optical measurements methods and digital image analysis (Schinagl et al., 1997; Wang et al., 2002). For example, in our recent study of immature bovine cartilage (Wang et al., 2002), we found  $E_Y \sim 100$  kPa and  $\nu \sim 0.05$  within 5% of the full-thickness depth from the articular surface, under an average tissue compressive strain of 10%. Accounting for differences in testing conditions, it seems reasonable to conclude that AFM measurements of  $E^*$  at the articular surface are consistent with these prior findings.

No major limitations were encountered in this study, as macroscopic measurements followed standard testing protocols while AFM measurements produced responses consistent with other materials. A minor limitation includes the use of the manufacturer's value for the AFM probe spring constant, although calibration studies conducted in house indicate no more than a 10% deviation from this rated value. Another minor limitation is that the range of normal forces used in the Hertz indentation analysis was a factor of two smaller than the full range of indentation forces used in the frictional measurements, though this has no effect on the main conclusions of the study. It should be noted that cartilage friction measurements with AFM may be dependent on the size of the scan area when it is below  $50 \times 50$   $\mu\text{m}$ . It is also reasonable to conclude that the measurement of friction force is not influenced by hydrodynamic forces on the spherical AFM probe tip.

In summary, the current study reports microscale AFM measurements of the friction coefficient of immature bovine articular cartilage in comparison with measurements at the macroscale level. To the best of our knowledge, these represent the first such measurements on articular cartilage in the literature. The main finding is that the AFM friction coefficient is more representative of the equilibrium friction coefficient reported at the macroscale, which represents the frictional response in the absence of cartilage interstitial fluid pressurization. These results suggest that AFM friction measurements may be highly suited for exploring the role of boundary lubricants in diarthrodial joint lubrication independently of the confounding effect of fluid pressurization. Such measurements may provide greater insight into the mechanism of articular cartilage lubrication.

#### Acknowledgements

This study was supported by funds from the National Institute of Arthritis and Musculoskeletal and Skin Diseases of the National Institutes of Health (AR-43628). We would like to thank Mr. Anil Rao

for conducting calibration measurements of the AFM probes.

## References

- A-Hassan, E., Heinz, W.F., Antonik, M.D., D'Costa, N.P., Nageswaran, S., Schoenenberger, C.A., Hoh, J.H., 1998. Relative microelastic mapping of living cells by atomic force microscopy. *Biophysical Journal* 74, 1564–1578.
- Armstrong, C.G., Lai, W.M., Mow, V.C., 1984. An analysis of the unconfined compression of articular cartilage. *Journal of Biomechanical Engineering* 106, 165–173.
- Ateshian, G.A., Lai, W.M., Zhu, W.B., Mow, V.C., 1994. An asymptotic solution for the contact of two biphasic cartilage layers. *Journal of Biomechanics* 27, 1347–1360.
- Ateshian, G.A., Wang, H., 1995. A theoretical solution for the frictionless rolling contact of cylindrical biphasic articular cartilage layers. *Journal of Biomechanics* 28, 1341–1355.
- Ateshian, G.A., 1997. A theoretical formulation for boundary friction in articular cartilage. *Journal of Biomechanical Engineering* 119, 81–86.
- Ateshian, G.A., Wang, H.Q., Lai, W.M., 1998. The role of interstitial fluid pressurization and surface porosities on the boundary friction of articular cartilage. *Journal of Tribology-Transactions of the ASME* 120, 241–248.
- Bhushan, B., 1995a. *Handbook of Micro/Nanotribology*. CRC Press, Boca Raton.
- Bhushan, B., 1995b. Micro/nanotechnology using atomic force microscopy/friction force microscopy: state of the art. *Proceedings of the Institution of Mechanical Engineers* 212 (J), 1–18.
- Bhushan, B., Koinkar, V.N., 1996. Nanoscale boundary lubrication studies using AFM/FFM. *Abstracts of Papers of the American Chemical Society*, Vol. 212, 239-Poly.
- Costa, K.D., Yin, F.C.P., 1999. Analysis of indentation: implications for measuring mechanical properties with atomic force microscopy. *Journal of Biomechanical Engineering-Transactions of the ASME* 121, 462–471.
- Dimitriadis, E.K., Horkay, F., Maresca, J., Kachar, B., Chadwick, R.S., 2002. Determination of elastic moduli of thin layers of soft material using the atomic force microscope. *Biophysical Journal* 82, 2798–2810.
- Du, B.Y., VanLandingham, M.R., Zhang, Q.L., He, T.B., 2001. Direct measurement of plowing friction and wear of a polymer thin film using the atomic force microscope. *Journal of Materials Research* 16, 1487–1492.
- Flannery, C.R., Hughes, C.E., Schumacher, B.L., Tudor, D., Aydelotte, M.B., Kuettner, K.E., Caterson, B., 1999. Articular cartilage superficial zone protein (SZP) is homologous to megakaryocyte stimulating factor precursor and is a multifunctional proteoglycan with potential growth-promoting, cytoprotective, and lubricating properties in cartilage metabolism. *Biochemical and Biophysical Research Communications* 254, 535–541.
- Forster, H., Fisher, J., 1996. The influence of loading time and lubricant on the friction of articular cartilage. *Proceedings of the Institution of Mechanical Engineers Part H* 210, 109–119.
- Forster, H., Fisher, J., 1999. The influence of continuous sliding and subsequent surface wear on the friction of articular cartilage. *Proceedings of the Institution of Mechanical Engineers Part H* 213, 329–345.
- Gong, J.P., Iwasaki, Y., Osada, Y., Kurihara, K., Hamai, Y., 1999. Friction of gels. 3. Friction on solid surfaces. *Journal of Physical Chemistry B* 103, 6001–6006.
- Grant, L.M., Tiberg, F., 2002. Normal and lateral forces between lipid covered solids in solution: correlation with layer packing and structure. *Biophysical Journal* 82, 1373–1385.
- Habelitz, S., Marshall, S.J., Marshall Jr., G.W., Balooch, M., 2001. The functional width of the dentino-enamel junction determined by afm-based nanoscratching. *J Struct Biol* 135, 294–301.
- Heinz, W.F., Hoh, J.H., 1999. Spatially resolved force spectroscopy of biological surfaces using the atomic force microscope. *Trends in Biotechnology* 17, 143–150.
- Hills, B.A., 2000. Boundary lubrication in vivo. *Proceedings of the Institution of Mechanical Engineers Part H-Journal of Engineering in Medicine* 214, 83–94.
- Hu, K., Radhakrishnan, P., Patel, R.V., Mao, J.J., 2001. Regional structural and viscoelastic properties of fibrocartilage upon dynamic nanoindentation of the articular condyle. *Journal of Structural Biology* 136, 46–52.
- Jay, G.D., Tantravahi, U., Britt, D.E., Barrach, H.J., Cha, C.J., 2001. Homology of lubricin and superficial zone protein (SZP): products of megakaryocyte stimulating factor (MSF) gene expression by human synovial fibroblasts and articular chondrocytes localized to chromosome 1q25. *Journal of Orthopaedic Research* 19, 677–687.
- Johnson, K.L., 1985. *Contact Mechanics*. Cambridge University Press, Cambridge, Cambridge, New York.
- Jurvelin, J.S., Muller, D.J., Wong, M., Studer, D., Engel, A., Hunziker, E.B., 1996. Surface and subsurface morphology of bovine humeral articular cartilage as assessed by atomic force and transmission electron microscopy. *Journal of Structural Biology* 117, 45–54.
- Kelkar, R., Ateshian, G.A., 1999. Contact creep of biphasic cartilage layers. *Journal of Applied Mechanics, Transactions ASME* 66, 137–145.
- Kim, S.H., Marmo, C., Somorjai, G.A., 2001. Friction studies of hydrogel contact lenses using AFM: non-crosslinked polymers of low friction at the surface. *Biomaterials* 22, 3285–3294.
- Kim, S.H., Opdahl, A., Marmo, C., Somorjai, G.A., 2002. AFM and SFG studies of pHEMA-based hydrogel contact lens surfaces in saline solution: adhesion, friction, and the presence of non-crosslinked polymer chains at the surface. *Biomaterials* 23, 1657–1666.
- Krishnan, R., Kopacz, M., Ateshian, G., 2003. Verification of the role of interstitial fluid load support in the frictional response of bovine articular cartilage. *Transactions of the Orthopedic Research Society* 28, 0287.
- Kumar, P., Oka, M., Toguchida, J., Kobayashi, M., Uchida, E., Nakamura, T., Tanaka, K., 2001. Role of uppermost superficial surface layer of articular cartilage in the lubrication mechanism of joints. *Journal of Anatomy* 199, 241–250.
- Malcom, L.L., 1976. An experimental investigation of the frictional and deformational response of articular cartilage interfaces to static and dynamic loading. Ph.D. Thesis, University of California, San Diego.
- Mathur, A.B., Truskey, G.A., Reichert, W.M., 2000. Atomic force and total internal reflection fluorescence microscopy for the study of force transmission in endothelial cells. *Biophysical Journal* 78, 1725–1735.
- Mathur, A.B., Collinsworth, A.M., Reichert, W.M., Kraus, W.E., Truskey, G.A., 2001. Endothelial, cardiac muscle and skeletal muscle exhibit different viscous and elastic properties as determined by atomic force microscopy. *Journal of Biomechanics* 34, 1545–1553.
- McCutchen, C.W., 1962. The frictional properties of animal joints. *Wear* 5, 1–17.
- McMullen, R.L., Kelty, S.P., 2001. Investigation of human hair fibers using lateral force microscopy. *Scanning* 23, 337–345.
- Meyer, G., Amer, N.M., 1990. Simultaneous measurement of lateral and normal forces with an optical-beam-deflection atomic force microscope. *Applied Physics Letters* 57, 2089–2091.
- Moa-Anderson, B.J., Costa, K.D., Hung, C.T., Ateshian, G.A., 2003. Bovine articular cartilage surface topography and roughness in

- fresh versus frozen tissue samples using atomic force microscopy. Proceedings of 2003 Summer Bioengineering Conference, paper 0561.
- Mow, V.C., Kuei, S.C., Lai, W.M., Armstrong, C.G., 1980. Biphasic creep and stress relaxation of articular cartilage in compression? theory and experiments. *Journal of Biomechanical Engineering* 102, 73–84.
- Mow, V.C., Ateshian, G.A., 1997. Lubrication and wear of diarthrodial joints. In: Mow, V.C., Hayes, W.C. (Eds.), *Basic Orthopaedic Biomechanics*. Lippincott-Raven, Philadelphia, pp. 275–315.
- Park, S., Krishnan, R., Nicoll, S.B., Ateshian, G.A., 2003. Cartilage interstitial fluid load support in unconfined compression. *Journal of Biomechanics* 36, 1785–1796.
- Patel, R.V., Mao, J.J., 2003. Microstructural and elastic properties of the extracellular matrices of the superficial zone of neonatal articular cartilage by atomic force microscopy. *Frontiers in Bioscience* 8, A18–A25.
- Poon, C.Y., Bhushan, B., 1995. Comparison of surface roughness measurements by stylus profiler, AFM and non-contact optical profiler. *Wear* 190, 76–88.
- Radmacher, M., 2002. Measuring the elastic properties of living cells by the atomic force microscope. In: Jena, B.P., Heinrich Hörber, J.K. (Eds.), *Atomic Force Microscopy in Cell Biology*. Academic Press, Amsterdam, pp. 67–90.
- Ruan, J.A., Bhushan, B., 1994. Atomic-scale friction measurements using friction force microscopy 0.1. General-principles and new measurement techniques. *Journal of Tribology-Transactions of the Asme* 116, 378–388.
- Schinagl, R.M., Gurskis, D., Chen, A.C., Sah, R.L., 1997. Depth-dependent confined compression modulus of full-thickness bovine articular cartilage. *Journal of Orthopaedic Research* 15, 499–506.
- Schumacher, B.L., Hughes, C.E., Kuettner, K.E., Caterson, B., Aydelotte, M.B., 1999. Immunodetection and partial cdna sequence of the proteoglycan, superficial zone protein, synthesized by cells lining synovial joints. *Journal of Orthopaedic Research* 17, 110–120.
- Soltz, M.A., Ateshian, G.A., 1998. Experimental verification and theoretical prediction of cartilage interstitial fluid pressurization at an impermeable contact interface in confined compression. *Journal of Biomechanics* 31, 927–934.
- Soltz, M.A., Ateshian, G.A., 2000a. Interstitial fluid pressurization during confined compression cyclical loading of articular cartilage. *Annals Biomedical Engineering* 28, 150–159.
- Soltz, M.A., Ateshian, G.A., 2000b. A conewise linear elasticity mixture model for the analysis of tension-compression nonlinearity in articular cartilage. *Journal of Biomechanical Engineering* 122, 576–586.
- Suh, N.P., Sin, H.C., 1981. The genesis of friction. *Wear* 69, 91–114.
- Swann, D.A., Silver, F.H., Slayter, H.S., Stafford, W., Shore, E., 1985. The molecular structure and lubricating activity of lubricin isolated from bovine and human synovial fluids. *Biochemical Journal* 225, 195–201.
- Tymiak, N.I., Kramer, D.E., Bahr, D.F., Wyrobek, T.J., Gerberich, W.W., 2001. Plastic strain and strain gradients at very small indentation depths. *Acta Materialia* 49, 1021–1034.
- Wang, C.C., Deng, J.M., Ateshian, G.A., Hung, C.T., 2002. An automated approach for direct measurement of two-dimensional strain distributions within articular cartilage under unconfined compression. *Journal of Biomechanical Engineering* 124, 557–567.